Real-Space Imaging of the Conformation and Atomic Structure of Individual β-Cyclodextrins with Noncontact AFM

Márkó Grabarics[1,2], Benjamín Mallada[3,4], Shayan Edalatmanesh[3,4], Alejandro Jiménez-Martín[3,4,5], Martin Pykal[4], Martin Ondráček[3], Petra Kührová[4], Weston B. Struwe[1,6], Pavel Banáš[4]*, Stephan Rauschenbach[1,2]*, Pavel Jelínek[3,4]* & Bruno de la Torre[4,7]*

M.G., B. M., and Sh. E. contributed equally.

[1]University of Oxford, Department of Chemistry, South Parks Road, Oxford OX1 3QU, UK

[2]Kavli Institute for Nanoscience Discovery, University of Oxford, Oxford, OX1 3QU, UK

[3]Institute of Physics, Czech Academy of Sciences; 16200 Prague, Czech Republic

[4]Czech Advanced Technology and Research Institute, Palacký University Olomouc, 78371 Olomouc, Czech Republic

[5]Faculty of Nuclear Sciences and Physical Engineering, Czech Technical University in Prague, Brehova 7, 115 19 Prague 1, Czech Republic

[6]University of Oxford, Department of Biochemistry, Oxford, OX1 3QU, UK

[7]Nanomaterials and Nanotechnology Research Center, CSIC-UNIOVI-PA, 33940 El Entrego, Spain

*Corresponding authors: bruno.de@upol.cz; pavel.banas@upol.cz; jelinekp@fzu.cz; stephan.rauschenbach@chem.ox.ac.uk

ABSTRACT: Glycans, consisting of covalently linked sugar units, are a major class of biopolymers essential to all known living organisms. To better understand their biological functions and further applications in fields from biomedicine to materials science, detailed knowledge of their structure is essential. However, due to the extraordinary complexity and conformational flexibility of glycans, state-of-the-art glycan analysis methods often fail to provide structural information with atomic precision. Here, we combine electrospray deposition in ultra-high vacuum with noncontact atomic force microscopy and theoretical calculations to unravel the structure of β-cyclodextrin, a cyclic glucose oligomer, with atomic-scale detail. Our results, established on the single-molecule level, reveal the different adsorption geometries and conformations of β-cyclodextrin. The cyclic arrangement of hydroxy groups on both faces of the molecule and the stabilizing H-bonds are imaged with atomic resolution, enabling the unambiguous assignment of the molecular structure and demonstrating the potential of the method for glycan analysis.

INTRODUCTION

Glycans are present in all cells, playing key roles in a range of biological processes and contributing greatly to the molecular and functional diversity of living organisms[1, 2]. Structurally, they consist of monosaccharide building blocks, such as glucose, mannose, and galactose, which are connected to each other *via* their OH groups, forming glycosidic linkages. Much of the structural diversity of glycans stems from variations in the orientation of these OH groups. Such variations lead to the isomerism of monosaccharide units, and the variability in the orientation of the glycosidic bonds between them. Combined with differences in linkage position, these small variations lead to the intrinsic and significant structural complexity of glycans. As minute structural differences can fine-tune biological function, analytical approaches sensitive to such small structural details and capable of revealing the underlying structure of glycans are highly sought after[3].

This immense complexity of glycans impedes complete structural assignments. Their elaborate regio- and stereochemistry pose significant challenges to state-of-the-art mass spectrometric methods[4, 5]. Isomers with identical masses are difficult to distinguish as they usually display very similar mass spectrometric fragmentation patterns, and the *de novo* assignment of linkage positions is hindered by the scarcity of diagnostic cross-ring fragments. In addition, atomic-resolution imaging of glycans by ensemble-averaged microscopic and diffraction methods is often not possible due to their conformational flexibility. Consequently, our knowledge of the structure of glycans is often incomplete, which represents a major bottleneck in better understanding their functions and facilitating their applications, from vaccine and drug development to materials science[6-10].

A novel approach to fully characterise the structure of glycans is based on the combination of electrospray ionisation based deposition methods and scanning tunnelling microscopy (STM), which enables the gentle deposition of the thermolabile glycans onto clean single crystal surfaces, and subsequent real-space imaging at the single-molecule level[11-16]. To obtain images with sufficient quality that allow for visualizing the connectivity of monosaccharide units within glycans, measurements must be performed under highly controlled conditions, requiring ultrahigh vacuum (UHV), cryogenic temperatures, and atomically flat surfaces. However, STM images obtained with bare metal tips reveal the overall shape of individual monosaccharide building blocks convoluted with their adsorption configuration[11, 17], while internal structural details at the atomic level remain unresolved.

Here we employ dynamic noncontact atomic force microscopy (nc-AFM) with CO-functionalized tips – enabled by electrospray deposition (ESD) of the molecules – to reveal the internal structure of monosaccharide units and resolve atomic-scale features that reflect individual functional groups and chemical bonds within the glycans. We investigate β-cyclodextrin (β-CD) as a model compound, a cyclic oligosaccharide consisting of seven D-glucopyranose units connected *via* α-1,4-glycosidic bonds (Fig. 1a). The shape of this macrocycle resembles a truncated cone where the glucose units enclose a central hydrophobic cavity[18]. Fourteen secondary OH groups form a wider rim at the cone's base (secondary face), while seven primary OH groups form a narrower rim at the top (primary face). Its three-

dimensional shape renders β-CD a challenging molecule for nc-AFM and expands the scope of this technique which has so far been applied mainly to conjugated planar molecular structures[19-23]. By combining experiments with nc-AFM simulations that also take electrostatic tip-molecule interactions into account, we show that the obtained images contain sufficient information to distinguish and unambiguously assign the different OH groups within single β-CD molecules, and to confidently identify the atomic structure and conformation of this complex biomolecule.

RESULTS & DISCUSSION

Identification of β-cyclodextrin conformers *via* single-molecule imaging

Incompatible with conventionally used thermal sublimation methods, β-CD was deposited onto an atomically clean Au(111) single crystal substrate at room temperature using ESD. Low-temperature STM topographs of the samples reveal irregular two-dimensional islands with average topographic heights between 250 and 350 pm (Fig. 1c and Fig. S1 in the Supplementary Information, SI). Within the islands, single β-CD molecules emerge as bright, doughnut-shaped objects. They consist of seven clearly resolved rounded lobes that encircle a central depression, which can be tentatively assigned to the individual glucose building blocks and the molecule's cavity, respectively. The β-CDs are surrounded by a lower bed of smaller fragments (shown in Fig. S2 in more detail), which most probably stem from the dissociation of the macrocycles during ESD, where electrochemical phenomena in ESD and collisions with the surface could both contribute to fragmentation.

Although STM reveals overall shapes and monomer units, a much more precise assignment can be achieved using high-resolution nc-AFM. Primarily, three dominant types of objects are identified on the surface, all illustrated in Fig. 1b. The first type (Fig. 1b, left panel) exhibits 7-fold symmetry with an outside diameter of 12.6 ± 0.5 Å. It features a central heptagon with bright, distinct borders enclosing a darker interior. A narrow ray points outwards from each corner of the heptagon, with darker regions between them, resulting in a star-shaped structure. This structure is surrounded by a faint, diffuse halo that gradually dissipates into the substrate's background. The second type (Fig. 1b, middle) appears larger across (15.6 ± 0.1 Å). Seven round features, separated by narrow ribs, are arranged in a circular pattern around a central cavity. The differences in their diameter (12.6 *v*. 15.6 Å), along with their similar absorption height relative to the substrate (roughly 7.5-8 Å, see Fig. S3), suggest that they correspond to two β-CD geometries on the surface.

The truncated cone shape of β-CD with its two distinct faces allows for two orientations on the surface where all seven glucose units are equally visible by STM. In one case, β-CD is adsorbed on the surface *via* its secondary face, the primary face with its narrow rim pointing upwards (primary face up or **p**↑ orientation). In the other case, the secondary face with the wide rim faces the probe, while the primary face points towards the surface (secondary face

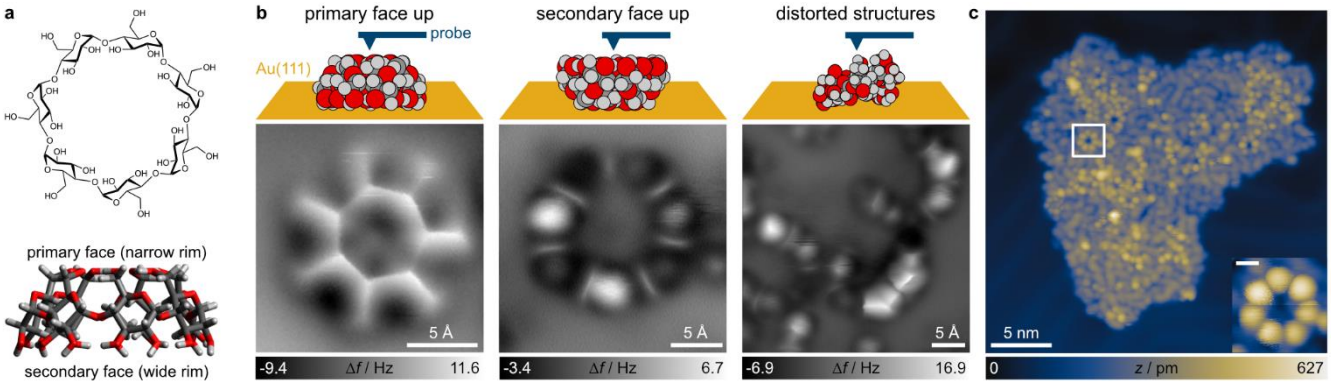

Fig 1. | Structure and real-space images of β-cyclodextrin molecules by low-temperature STM and nc-AFM. a, Chemical formula of β-CD and side-view of a 3D-model highlighting the molecule's truncated cone shape. **b,** nc-AFM images of β-CD on Au(111), recorded at constant height using frequency modulation detection. Representative examples are shown for the primary and secondary face up geometries, as well as for distorted molecules. **c,** STM overview showing an irregular island formed upon electrospray deposition of β-CD onto Au(111) (bias = 1 V, tunnelling current = 1 pA). The macrocycles stand out as doughnut-shaped structures from a lower background of fragments; the insert shows a higher-resolution STM image of a single macrocycle (scale bar in insert is 5 Å).

up or **s**↑). Accordingly, based on the different diameters observed, the star-shaped objects are assigned to **p**↑, while the larger ones to the **s**↑ orientation. The assignment is further confirmed by simulated nc-AFM images of both geometries (discussed further in the next section).

The third frequently observed object corresponds to distorted β-CD molecules (Fig. 1b, right panel). In this case, only a few of the round features observed in molecules in **s**↑ orientation can be resolved. Upon comparison with simulated nc-AFM images (see Fig. S5), it becomes evident that these correspond to bent β-CD molecules, where only outward-facing features are visible in the constant-height nc-AFM images. Molecular dynamics simulations revealed that such distortion arises from the rotation of two α-1,4-glycosidic bonds, breaking the symmetry of the β-CD molecules (for more details see Section 4 in the SI). This rotation causes two adjacent glucose units to twist, with their glucopyranose rings stacked on the surface. The remaining five glucose units remain in the original conformation. This conformational substate of the β-CD molecule was found to be a minor population in free solvent simulations. However, it is significantly stabilized when the β-CD molecule is adsorbed on the surface in the **s**↑ orientation.

The nc-AFM images were recorded in constant-height mode using frequency modulation detection. In this detection mode, more positive Δf frequency shifts (depicted in bright grey) reflect enhanced repulsive forces between the CO molecule attached to the tip and the molecule on the surface[24, 25]. The repulsion arises mainly from the steric Pauli repulsion at close tip-sample distances and alternatively from the electrostatic interaction. Thus, in the first approximation, we may interpret bright areas as regions of higher electron density within the molecules, often indicating the location of atoms and chemical bonds[26]. Dark areas, in contrast, correspond to regions with attractive interaction driven by long-range van der Waals and, alternatively, electrostatic interactions dominating over short-range steric repulsion. Considering these contrast mechanisms in nc-AFM, some tentative structural assignments may be made based on the experimental micrographs. In **p**↑, for instance, the bright borders of the heptagon, which outline a sharp ridge on the potential energy surface above the

molecule, indicate the presence of a closed H-bonding network along the narrow rim of β-CD. In the case of **s**↑, the seven round features and ribs must arise from corresponding atomic groups of the seven glucose building blocks, which very likely involve the secondary OH groups. However, unambiguous identification of the exact atoms giving rise to these features or determining the ring puckers of the glucopyranose units is not possible based solely on the singular constant-height images. The characteristics of nc-AFM images are dominated by forces that change with the tip-sample distance. Thus, for more definite structural assignments, experimental micrographs acquired at different tip-sample distances were compared to simulated images for a set of low-energy structural candidates.

Structural assignment with atomic-scale detail – comparison of experiment and theory

The precise structural arrangement of different β-CD conformers from high-resolution nc-AFM imaging was elucidated through comparison with simulated nc-AFM images using the probe-particle (PP) model[24]. In essence, the probe particle (here a CO molecule) positioned at the tip apex demonstrates sensitivity to spatial fluctuations in the potential energy landscape of the molecule, arising from the interplay among Pauli, electrostatic, and van der Waals interactions[27-29]. At short distances between the tip and sample, the probe particle adjusts in response to the potential energy surface, generating a distinct sub-molecular contrast. For modelling the sample, a set of low-energy gas-phase β-CD conformers were generated by classical MD simulations and subsequently relaxed on the Au(111) surface in both **p**↑ and **s**↑ geometry. Equilibrated molecules on the Au(111) surface were then used for additional total energy density functional theory (DFT) calculations using FHI-aims.[30]

Fig. 2 compares theoretical and experimental nc-AFM images acquired for the **p**↑ geometry. The optimized atomic model of the conformer of β-CD using total energy DFT calculations, which gave the most accurate match between simulations and experimental images, is shown from the side of its primary face in Fig. 2a (atomic coordinates provided as part of the SI). The most important functional groups are highlighted in the figure in colour, and the numbering of atoms is explained in the SI in more detail (see Fig. S8). The structure in Fig. 2a exhibits C_7 symmetry with all glucopyranose units adopting a $^4C_1$ ring pucker. Along the narrow rim of the primary face a closed, homodromic H-bonding network is formed by the seven primary C6-OH groups (OH···O distances at 1.79 Å), all serving both as donor and acceptor. In both experiment and simulation, the resulting ridges in the interaction potential energy surface above the molecule in **p**↑ orientation become visible at close tip-sample distances as the sharp borders of the central heptagon (Fig. 2b). The gradual emergence, size, and symmetry of the seven rays observed in experiments are also accurately reproduced in the simulations, along with the position and contrast of the darker regions. Overall, the agreement between experimental and simulated nc-AFM images is highly accurate for the **p**↑ geometry. Overlay of the atomic model with a corresponding simulated image for **p**↑ also enables direct visual assignment (Fig. 2c). As mentioned above, the structural elements underlying the central heptagon are the primary C6-OH groups that form a closed network of H-bonds. This also suggests that β-CD may be present as neutral species on the Au(111) surface following

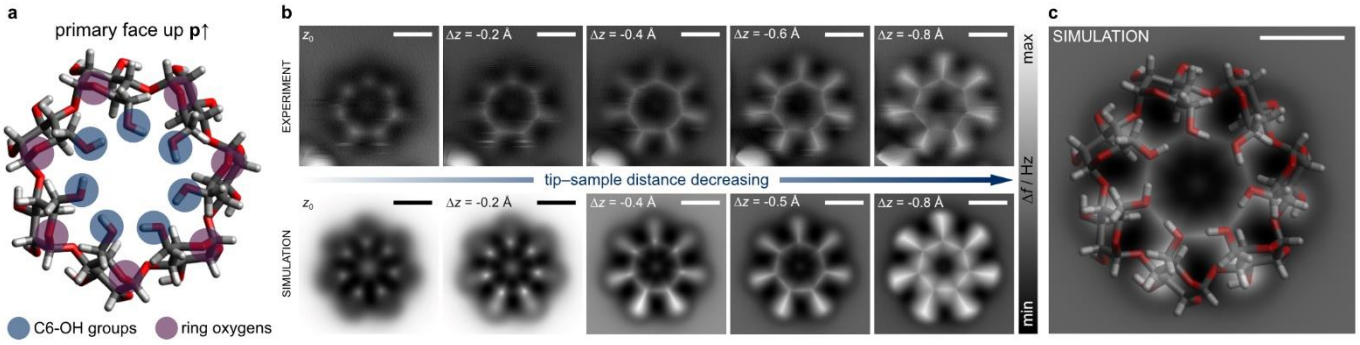

Fig 2. | Comparison of experimental and simulated nc-AFM images of the β-cyclodextrin primary face. a, Atomic model of β-CD, representing the lowest-energy conformer at the DFT PBE level of theory, viewed from its primary face. More prominent functional groups are highlighted in colour for ease of discussion. **b,** Experimental (top) and simulated (bottom) nc-AFM images of β-CD in the **p**↑ geometry, the tip-sample distance decreasing from left to right. In the experiment z_0 is defined as +250 pm relative to an initial STM setpoint with the feedback at 1 V and 3 pA. **c,** Overlay of atomic model and corresponding simulated image of β-CD in the **p**↑ geometry; the exact atomic groups giving rise to the various features can be readily identified. All scale bars are 5 Å.

electrospray deposition, as coordination to small metal ions – potentially present in the electrosprayed solutions – generally disrupts the regular intramolecular H-bonding pattern in isolated cyclodextrins.[31] The seven rays can be assigned mainly to the methylene bridges that connect the C6-OH groups with the six-membered pyranose rings of the glucose units. The ring oxygens located an atomic layer below, and the glycosidic oxygens, buried even deeper, are not directly visible in the images. These results show the superior resolution and additional structural information provided by nc-AFM as compared to conventional STM, where such assignments would be impossible due to lack of high-resolution, sub-monomer detail.

A similar comparison of experiment and simulation for the **s**↑ geometry is shown in Fig. 3. Here, the structural elements most accessible to the tip are the secondary OH groups, highlighted in colour in Fig. 3a. These groups point anti-clockwise when seen from the secondary face, forming H-bonds in a pairwise manner along the wide rim where the C3-OH oxygens (O3) serve as donors and the C2-OH oxygens (O2) as acceptors. Simulated images for **s**↑ are also in excellent agreement with their experimental counterparts (Fig. 3b). The central cavity, the round features, and the narrow ribs observed experimentally are all correctly reproduced by theory at different tip-sample distances. By overlaying the atomic model on the corresponding simulated images, the seven round features and the seven ribs can be assigned to the C2-OH and C3-OH groups, respectively. Overall, the agreement between experiment and simulation is very convincing for both adsorption geometries, enabling a confident assignment of β-CD's atomic structure.

It needs mentioning that the β-CD molecules in **s**↑ orientation appear slightly distorted in the experimental images. Variations in the brightness of the round features and ribs indicate that, upon adsorption *via* its primary face, β-CD can undergo slight deformation that leads to differences in the height of the secondary OH groups (typically within the fraction of an Å). While comparable variations in conformation may prevent ensemble-averaged imaging methods from obtaining high-resolution structural information, nc-AFM allows for the

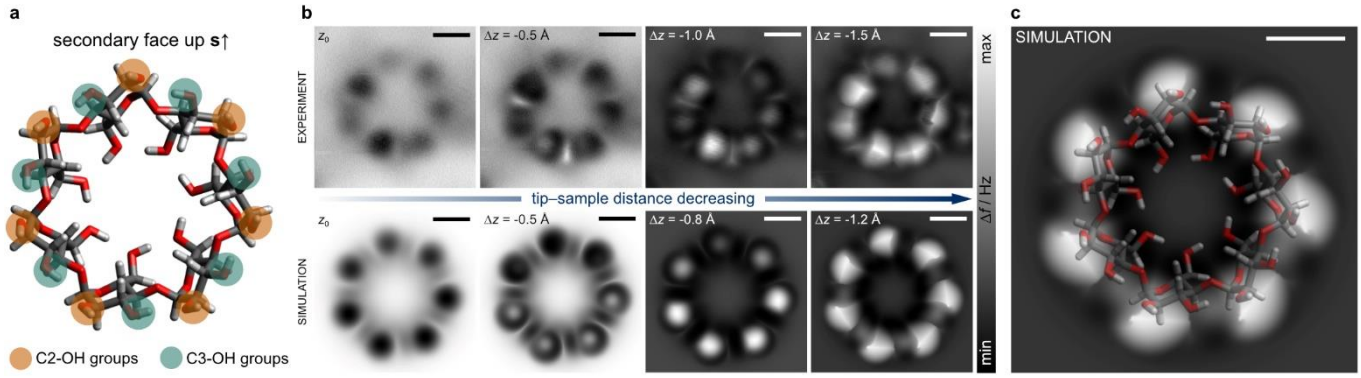

Fig 3. | Comparison of experimental and simulated nc-AFM images of the β-cyclodextrin secondary face. a, Atomic model of β-CD, representing the lowest-energy conformer at the DFT PBE level of theory, viewed from its secondary face. More prominent functional groups are highlighted in colour. **b,** Experimental (top) and simulated (bottom) nc-AFM images of β-CD in the **s**↑ geometry, the tip-sample distance decreasing from left to right. In the experiment z_0 is defined as +190 pm relative to an initial STM setpoint with the feedback at 0.5 V and 1 pA. **c,** Overlay of atomic model and corresponding simulated image of β-CD in the **s**↑ geometry. All scale bars are 5 Å.

imaging of single molecules in real space, thereby revealing the structural heterogeneity present in the sample.

Besides enabling the assignment of β-CD's atomic structure, simulations also helped provide rationale behind the observed contrast in the nc-AFM images. Notably, we found improved agreement between theoretical and experimental nc-AFM images when the electrostatic interaction between tip and sample was taken into account. The impact of electrostatics on the simulated images is shown in Fig. 4 for the **s**↑ orientation. The influence of electrostatics is also recognizable for **p**↑ (see Fig. S7), but is much more prominent in the case of the **s**↑ geometry. The greater impact of the electrostatic interaction on the latter reflects the stronger polar character of the secondary face. This results mainly from differences in the orientation and bonding of the C2-OH and C3-OH groups, which also contribute to their different contrast. The hydrogens of the C2-OH groups in the atomic model point away from the plane of the O2 atoms, protruding slightly from the secondary face. The hydrogens in the C3-OH groups, on the other hand, are located in the plane of the O2 atoms, with which they engage in H-bonds. Thus, the hydrogen atoms in the C2-OH groups are located somewhat closer to the plane of the tip. As the O-H bonds are highly polar, the difference in the orientation of the C2-OH and C3-OH groups leads to an alternating pattern of positive and negative electrostatic potential values above these moieties (see the electrostatic potential maps in Fig. 4e and j). The resulting difference in the electrostatic interaction, combined with variations in steric repulsion, are largely responsible for the different contrast of the two sets of secondary OH groups. These findings highlight the sensitivity of nc-AFM to small differences in the orientation and chemical environment of otherwise very similar functional groups within a complex glycan structure.

Fig. S6 shows simulated nc-AFM images for other stable and symmetric β-CD conformers from MD simulations, which display a different orientation of the hydroxy groups. However, these simulated images show significantly different sub-molecular contrast compared to the experiments, which further demonstrates the power of nc-AFM to identify atomic structural differences, in particular molecular conformations. Considering these findings, it is tempting

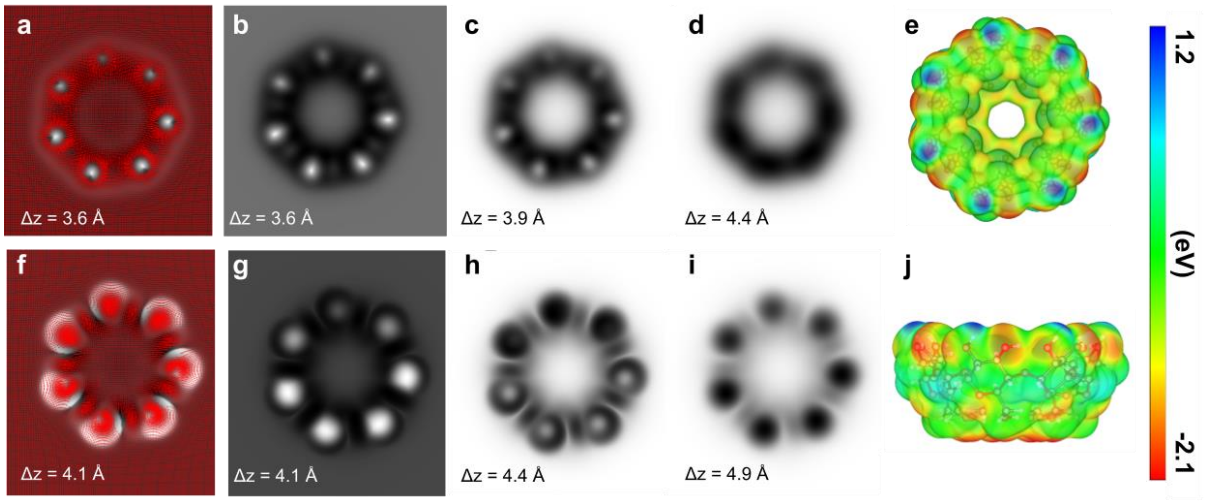

Figure 4. DFT-calculated nc-AFM simulations and the electrostatic potential of β-cyclodextrin with its secondary face upwards. The lateral relaxations of CO-like probe particle at tip-sample distances corresponding to simulated nc-AFM images **b** and **g** are presented as red dots in panels **a** and **f**, respectively. Panels **b–d** hold the nc-AFM simulations without including the electrostatic potential, and sections **g–i** contain the simulations that include the electrostatic interaction between probe and sample. Panels **e** and **j** include the top (viewed from the secondary face) and side views of β-CD's electrostatic potential map, respectively.

to envisage similar sensitivity in identifying conformers and isomeric species from other glycan classes by nc-AFM, or even other biomolecules of comparable size. As a method capable of providing atomic-level structural detail for complex, three-dimensional biomolecular species on the single-molecule level as demonstrated herein, nc-AFM in combination with ESD has the potential to overcome many of the key challenges associated with glycan analysis, complement established analytical methods, and significantly improve our understanding of the structure of glycans and other biomolecules.

CONCLUSION

This work demonstrates the high-resolution imaging of single glycan molecules using nc-AFM with CO-functionalized probes, providing atomic-level structural information on β-CD, a complex biomolecule with a distinctive three-dimensional shape. Compared to conventional STM methods, nc-AFM displays superior spatial resolution that reveals the internal structure of the monosaccharide building blocks. Individual OH groups and intramolecular H-bonding interactions – most prominently a closed H-bonding network of the C6-OH groups on the primary face – are resolved on the level of single bonds. By combining nc-AFM experiments with first-principles DFT simulations, the strong dependence of the imaging contrast on minor variations in the position and chemical environment of the secondary OH groups could be rationalized, allowing the unambiguous distinction and assignment of these key structural elements. The strong agreement between experiment and theory, taking into account the different adsorption geometries of β-CD, allowed for the confident assignment of the molecule's atomic structure.

This study represents the first application of high-resolution nc-AFM for glycan analysis, and serves as a significant step towards extending this technique beyond the analysis of conjugated planar molecules. Our results also pave the way for further nc-AFM studies

exploring more complex glycans from both synthetic and natural sources. Determining conformations, distinguishing isomers, and assigning linkage position and configuration in unknown structures are key challenges where nc-AFM has the potential to complement established mass spectrometric and spectroscopic methods. The combination of nc-AFM with electrospray ion beam deposition (ESIBD)[32, 33] to enable the soft landing of mass-selected ionic species would open further possibilities, including the analysis of complex glycan mixtures or studies on fragments generated in gas-phase reactions. Based on the findings presented herein, we anticipate that nc-AFM will play an important role in advancing our understanding of the structure of glycans and other complex biomolecules.

ACKNOWLEDGEMENTS

M. P., P. K. and B. T. acknowledge the Research Infrastructure NanoEnviCz, supported by the Ministry of Education, Youth and Sports of the Czech Republic (MEYS CR) under Project No. LM2023066. M.G. acknowledges support from the DFG Walter Benjamin Programme (Project GR 6150/1-1). B. M., A. J.-M. and B.T. acknowledges the financial support of Czech Science Foundation 23-06781M. P.J., M.O., and Sh. E. acknowledge the financial support of Czech Science Foundation 20-13692X. W.S acknowledges support from the UKRI Future Leaders Fellowship [MR/V02213X/1]. W.S., S.R and M.G. acknowledge support from the UKRI BBSRC (project BB/W017024/1). M.O., Sh.E. and P.J. acknowledge computational resources provided by the e-INFRA CZ project (ID:90254), supported by MEYS CR.

METHODS

Simulation of nc-AFM images

The AFM probe was modelled as the outermost atom of the metal tip to which a CO molecule (the probe particle) is covalently attached *via* its C atom. Simulated images were obtained by laterally scanning this probe with a step size of 0.1 Å above the sample. At each lateral position, the probe was approached towards the sample in steps of 0.1 Å and allowed to relax. Following relaxation at each step, the vertical component of the force exerted on the probe by the sample was calculated and subsequently converted into Δf values. The simulated $\Delta f(x,y)$ maps were finally compared to those recorded experimentally. Further details of structural modelling and simulations are provided in the SI.

Electrospray deposition of β-cyclodextrin

For electrospray deposition (ESD), β-cyclodextrin (from Sigma-Aldrich, purity ≥97%) was dissolved in a 50:50 (*v*/*v*) mixture of water (Milli-Q®) and methanol (HPLC-grade, ≥99.9%) at a concentration of 1 mg/mL. The solution was then loaded into a gastight Hamilton syringe, connected to the emitter of a commercially available UHV4i ESD source[34] (Molecularspray Ltd.) through a PEEK capillary. To achieve stable spray conditions, the solution was pumped at a constant flow rate of 300 μL/h using a syringe pump, with the emitter held at a potential of +2.3 kV. The molecules were deposited onto the (111) surface of an Au single crystal

(MaTecK GmbH), held at room temperature in the UHV chamber of the microscope. During deposition, the pressure in the preparation chamber increased to the 10^{-7} mbar range from a base pressure of 10^{-9} mbar.

Low-temperature STM and nc-AFM experiments

The experiments were conducted at a temperature of 4.2 K using a commercial STM/nc-AFM microscope from CreaTec Fischer & Co. GmbH. Pt/Ir tips, sharpened by focused ion beam (FIB), were utilized and were further cleaned and shaped by gentle indentations (~1 nm) in the bare metallic substrate. The Au(111) substrate was prepared through repeated cycles of argon ion (Ar^+) sputtering at 1 keV, followed by annealing at approximately 800 K.

STM topography was acquired in constant current mode with the bias voltage applied to the sample. Due to the low conductivity of the β-cyclodextrins, constant current images were typically performed with very low tunnelling currents between 500 fA and 3 pA. In nc-AFM imaging, a qPlus sensor[35] (resonant frequency ≈ 30 kHz; stiffness ≈ 1800 N/m) was operated in frequency modulation mode with an oscillation amplitude of 50 pm.

The nc-AFM images were obtained in constant height mode using CO-terminated tips. The CO functionalization was performed by moving the tip in constant current to a CO molecule on the Au(111) surface with a setpoint of 20 pA tunnelling current and 50 mV bias voltage. Once over the CO molecule, the STM feedback loop is opened, and the tip is approached towards the CO until a sudden drop in current and a corresponding change in frequency shift were observed.

The STM/nc-AFM images were processed using Gwyddion[36], WSxM[37] and SpmImage Tycoon[38] software.

REFERENCES

1. Dwek RA. Glycobiology: Toward Understanding the Function of Sugars. *Chem Rev* 1996, **96:** 683-720.

2. Varki A. Biological roles of glycans. *Glycobiology* 2017, **27**(1)**:** 3-49.

3. Gray CJ, Migas LG, Barran PE, Pagel K, Seeberger PH, Eyers CE*, et al.* Advancing Solutions to the Carbohydrate Sequencing Challenge. *Journal of the American Chemical Society* 2019, **141**(37)**:** 14463-14479.

4. Ruhaak LR, Xu G, Li Q, Goonatilleke E, Lebrilla CB. Mass Spectrometry Approaches to Glycomic and Glycoproteomic Analyses. *Chem Rev* 2018, **118**(17)**:** 7886-7930.

5. Grabarics M, Lettow M, Kirschbaum C, Greis K, Manz C, Pagel K. Mass Spectrometry-Based Techniques to Elucidate the Sugar Code. *Chem Rev* 2022, **122**(8)**:** 7840-7908.

6. Ernst B, Magnani JL. From carbohydrate leads to glycomimetic drugs. *Nature Reviews Drug Discovery* 2009, **8:** 661.

7. Hudak Jason E, Bertozzi Carolyn R. Glycotherapy: New Advances Inspire a Reemergence of Glycans in Medicine. *Chem Biol* 2014, **21**(1)**:** 16-37.

8. Smith BAH, Bertozzi CR. The clinical impact of glycobiology: targeting selectins, Siglecs and mammalian glycans. *Nature Reviews Drug Discovery* 2021, **20**(3)**:** 217-243.

9. Seeberger PH. Discovery of Semi- and Fully-Synthetic Carbohydrate Vaccines Against Bacterial Infections Using a Medicinal Chemistry Approach. *Chem Rev* 2021, **121**(7)**:** 3598-3626.

10. Djalali S, Yadav N, Delbianco M. Towards glycan foldamers and programmable assemblies. *Nature Reviews Materials* 2024.

11. Abb S, Tarrat N, Cortés J, Andriyevsky B, Harnau L, Schön JC*, et al.* Carbohydrate Self-Assembly at Surfaces: STM Imaging of Sucrose Conformation and Ordering on Cu(100). *Angew Chem Int Ed* 2019, **58**(25)**:** 8336-8340.

12. Wu X, Delbianco M, Anggara K, Michnowicz T, Pardo-Vargas A, Bharate P*, et al.* Imaging single glycans. *Nature* 2020, **582**(7812)**:** 375-378.

13. Anggara K, Zhu Y, Delbianco M, Rauschenbach S, Abb S, Seeberger PH*, et al.* Exploring the Molecular Conformation Space by Soft Molecule–Surface Collision. *Journal of the American Chemical Society* 2020.

14. Anggara K, Zhu Y, Fittolani G, Yu Y, Tyrikos-Ergas T, Delbianco M*, et al.* Identifying the origin of local flexibility in a carbohydrate polymer. *Proceedings of the National Academy of Sciences* 2021, **118**(23)**:** e2102168118.

15. Anggara K, Sršan L, Jaroentomeechai T, Wu X, Rauschenbach S, Narimatsu Y*, et al.* Direct observation of glycans bonded to proteins and lipids at the single-molecule level. *Science* 2023, **382**(6667)**:** 219-223.

16. Seibel J, Fittolani G, Mirhosseini H, Wu X, Rauschenbach S, Anggara K*, et al.* Visualizing Chiral Interactions in Carbohydrates Adsorbed on Au(111) by High-Resolution STM Imaging. *Angew Chem Int Ed* 2023, **62**(39)**:** e202305733.

17. Abb S, Tarrat N, Cortés J, Andriyevsky B, Harnau L, Schön JC*, et al.* Polymorphism in carbohydrate self-assembly at surfaces: STM imaging and theoretical modelling of trehalose on Cu(100). *RSC Advances* 2019, **9**(61)**:** 35813-35819.

18. Szejtli J. Introduction and General Overview of Cyclodextrin Chemistry. *Chem Rev* 1998, **98**(5)**:** 1743-1754.

19. Gross L, Mohn F, Moll N, Meyer G, Ebel R, Abdel-Mageed WM*, et al.* Organic structure determination using atomic-resolution scanning probe microscopy. *Nat Chem* 2010, **2**(10)**:** 821-825.

20. Iwata K, Yamazaki S, Mutombo P, Hapala P, Ondráček M, Jelínek P*, et al.* Chemical structure imaging of a single molecule by atomic force microscopy at room temperature. *Nat Commun* 2015, **6**(1)**:** 7766.

21. Patera LL, Queck F, Repp J. Imaging Charge Localization in a Conjugated Oligophenylene. *Phys Rev Lett* 2020, **125**(17)**:** 176803.

22. Xu J, Zhu X, Tan S, Zhang Y, Li B, Tian Y*, et al.* Determining structural and chemical heterogeneities of surface species at the single-bond limit. *Science* 2021, **371**(6531)**:** 818-822.

23. de la Torre B, Švec M, Foti G, Krejčí O, Hapala P, Garcia-Lekue A*, et al.* Submolecular Resolution by Variation of the Inelastic Electron Tunneling Spectroscopy Amplitude and its Relation to the AFM/STM Signal. *Phys Rev Lett* 2017, **119**(16)**:** 166001.

24. Hapala P, Kichin G, Wagner C, Tautz FS, Temirov R, Jelínek P. Mechanism of high-resolution STM/AFM imaging with functionalized tips. *Physical Review B* 2014, **90**(8)**:** 085421.

25. Jelínek P. High resolution SPM imaging of organic molecules with functionalized tips. *J Phys: Condens Matter* 2017, **29**(34)**:** 343002.

26. Pavliček N, Gross L. Generation, manipulation and characterization of molecules by atomic force microscopy. *Nat Rev Chem* 2017, **1**(1)**:** 0005.

27. Moll N, Gross L, Mohn F, Curioni A, Meyer G. A simple model of molecular imaging with noncontact atomic force microscopy. *New Journal of Physics* 2012, **14**(8)**:** 083023.

28. Hapala P, Temirov R, Tautz FS, Jelínek P. Origin of High-Resolution IETS-STM Images of Organic Molecules with Functionalized Tips. *Phys Rev Lett* 2014, **113**(22)**:** 226101.

29. Hapala P, Švec M, Stetsovych O, van der Heijden NJ, Ondráček M, van der Lit J*, et al.* Mapping the electrostatic force field of single molecules from high-resolution scanning probe images. *Nat Commun* 2016, **7**(1)**:** 11560.

30. Blum V, Gehrke R, Hanke F, Havu P, Havu V, Ren X*, et al.* Ab initio molecular simulations with numeric atom-centered orbitals. *Comput Phys Commun* 2009, **180**(11)**:** 2175-2196.

31. Stachowicz A, Styrcz A, Korchowiec J, Modaressi A, Rogalski M. DFT studies of cation binding by β-cyclodextrin. *Theor Chem Acc* 2011, **130**(4)**:** 939-953.

32. Rauschenbach S, Vogelgesang R, Malinowski N, Gerlach JW, Benyoucef M, Costantini G*, et al.* Electrospray Ion Beam Deposition: Soft-Landing and Fragmentation of Functional Molecules at Solid Surfaces. *ACS Nano* 2009, **3:** 2901-2910.

33. Rauschenbach S, Ternes M, Harnau L, Kern K. Mass Spectrometry as a Preparative Tool for the Surface Science of Large Molecules. *Annu Rev Anal Chem* 2016, **9:** 473-498.

34. Satterley CJ, Perdigão LMA, Saywell A, Magnano G, Rienzo A, Mayor LC*, et al.* Electrospray deposition of fullerenes in ultra-high vacuum: in situ scanning tunneling microscopy and photoemission spectroscopy. *Nanotechnology* 2007, **18**(45)**:** 455304.

35. Giessibl FJ. The qPlus sensor, a powerful core for the atomic force microscope. *Rev Sci Instrum* 2019, **90**(1)**:** 011101.

36. Nečas D, Klapetek P. Gwyddion: an open-source software for SPM data analysis. 2012, **10**(1)**:** 181-188.

37. Horcas I, Fernández R, Gómez-Rodríguez JM, Colchero J, Gómez-Herrero J, Baro AM. WSXM: A software for scanning probe microscopy and a tool for nanotechnology. *Rev Sci Instrum* 2007, **78**(1)**:** 013705.

38. Riss A. SpmImage Tycoon: Organize and analyze scanning probe microscopy data. *Journal of Open Source Software* 2022, **7**(77)**:** 4644.